ORIGINAL PAPER

Angela Šurca · Boris Orel · Boris Pihlar

Characterisation of redox states of Ni(La)-hydroxide films prepared via the sol-gel route by *ex situ* IR spectroscopy

Abstract Ni(La)-hydroxide films were prepared from aqueous colloidal solutions containing nickel sulfate and lanthanum acetate in the molar ratio 10:1. Two types of film were made by heating for 15 and 60 min at 300 °C. Thermogravimetry (TG) and X-ray diffraction (XRD) reveal that both films consist of NiO (bunsenite 40%) nanoparticles (particle size ~30 Å), the remainder being amorphous. IR spectroscopy showed that the amorphous phase comprised the $\alpha(II)$-Ni(OH)$_2$ phase incorporating SO$_4^{2-}$, carboxylate and water species. Cyclic voltammetry (CV) in a 0.1 M LiOH electrolyte combined with in situ UV-VIS spectroscopy revealed that the colouring/bleaching changes, as a function of applied potential, differed considerably for the two types of film. Ex situ IR spectroelectrochemical measurements at near-grazing incidence angle conditions using P-polarised light (NGIA IR) were performed for films heated for 60 min in 0.1 M LiOH and 0.1 M tetramethylammonium hydroxide (TMAH) electrolytes and cycled 1402 and 1802 times. During the oxidation/reduction cycles the $\alpha(II)$-Ni(OH)$_2$ phase transforms to the $\gamma(III)$-NiOOH phase, while the $\beta(II)$-Ni(OH)$_2$ did not develop. This explains the high cycling stability of Ni(La)-hydroxide films. The incorporation of TMA$^+$ ions was observed from the $\nu(CH_3)$ stretching band intensities in the IR spectra of cycled films.

Key words Electrochromism · Sol-gel film · Nickel hydroxide · Lanthanum · IR spectroscopy · UV-visible spectroscopy
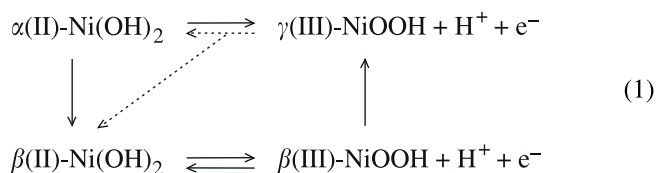
A. Šurca · B. Orel (✉)
National Institute of Chemistry, Hajdrihova 19, SI-1001 Ljubljana, Slovenia
Tel.: +386 61 17 60 200 or +386 61 17 60 276
Fax: +386 61 12 59 244; e-mail: boris.orel@ki.si

B. Pihlar
Faculty of Chemistry and Chemical Technology, Aškerčeva 5, SI-1000 Ljubljana, Slovenia

Introduction

Nickel hydroxide electrodes have been the subject of numerous studies because of their use in Ni-Cd, Ni-Fe and Ni-Zn alkaline batteries [1–3]. Additionally, this material has an inherent ability to reversibly change colour from transparent to deep brown under the application of a voltage, i.e., it shows anodic electrochromism [4]. Thus, in the thin-film form it can be used in an electrochromic (EC) device with a complementary colouring cathodic electrochromic material like WO$_3$ [5], or in an EC device where optically passive ion-storage films (CeO$_2$, SnO$_2$,...) are used as counter electrodes [6–8]. The change in optical density (ΔOD) between the coloured and bleached states of nickel hydroxide film per inserted/extracted charge (ΔQ) (i.e., the coloration efficiency $\eta = \Delta$OD$/\Delta Q$) exceeds 30 cm^2 C^{-1} [9], while the changes in transmittance are up to 50% [9, 10].

The main drawback to the practical application of nickel hydroxide films in EC devices is the gradual transformation of the amorphous $\alpha(II)$-Ni(OH)$_2$ phase (during the potential cycling in protic electrolytes) to the $\beta(II)$-Ni(OH)$_2$ phase according to the Bode scheme [11]:

$$\alpha(II)\text{-Ni(OH)}_2 \rightleftharpoons \gamma(III)\text{-NiOOH} + H^+ + e^-$$

$$\tag{1}$$

$$\beta(II)\text{-Ni(OH)}_2 \rightleftharpoons \beta(III)\text{-NiOOH} + H^+ + e^-$$

In general (see Eq. 1), in undoped $\alpha(II)$ films the $\beta(II)$ phase develops during cycling. In the $\beta(II)$ phase, which is reversibly transformed to the $\beta(III)$-NiOOH phase with the application of anodic potentials, the expansion (contraction) of the brucite-type sheets upon oxidation (reduction) of about 15% adversely affects the cycling stability of the $\beta(II)$ phase [1]. Over long periods of cycling, and especially when in a strong alkaline electrolyte, the $\beta(III)$ phase irreversibly transforms to the more expanded $\gamma(III)$-NiOOH phase from which the $\beta(II)$

phase can no longer be formed [1]. This suggests that the films that show cycling stability are those in which the $\beta(II)/\beta(III)$ phases do not develop during prolonged cycling.

The formation of novel phases has been reported by numerous workers studying $Ni(OH)_2$ powders [12–14]. Also, thin films prepared by sputtering [15–17], e-beam evaporation [18, 19], thermal decomposition [20], electrodeposition [10, 21, 22] and sol-gel deposition [23] have been studied. Recently, we noted that sol-gel-derived Ni-hydroxide films prepared from nickel sulfate precursors with organic additives (polyvinyl alcohol – PVA, formamide, glycerol), containing up to 40% of the electrochemically inactive NiO (bunsenite) phase and approximately 60% of amorphous $\alpha(II)$ phase, exhibited good electrochemical stability (200 cycles) and large electrochromic colouring/bleaching changes (up to 60%) [24, 25]. The mechanical resistance and adhesion properties of films were improved by making Ni(Si)-hydroxide films prepared from nickel sulfate precursor and 3-aminopropyltrimethoxysilane [26]. Extensive IR spectroscopic investigations of as-deposited and cycled Ni(Si)-hydroxide films allowed the detection of all the phases predicted by the Bode scheme (Eq. 1), including the identification of the expanded $\gamma(III)$ phase.

Improvements in the cycling stability of the $\alpha(II)/\gamma(III)$ redox pair have been attained by the addition of Co [3, 27–29]. Other metal ions such as Fe, Mn, Al, La, Ce have also been tested [30–35]. Recently, Mo et al. [33], from the measured quartz crystal microbalance (QCM) response of Ni-hydroxide and Ni/Co-hydroxide films, reported that Co-containing films prepared by electrodeposition do not exhibit structural changes from the original $\alpha(II)$ to $\beta(II)$ phase. The influence of Co, which prevents or significantly retards the structural changes in pure $\alpha(II)$ films, was also observed by Faure et al. [3, 27–29]. However, IR spectroscopic evidence for the development of the $\beta(II)/\beta(III)$ phases in nickel hydroxide films, in relation to their cycling stability originating from added ions, does not appear in the literature.

Corrigan et al. [34] found that Co/La/Ni-hydroxide films prepared by cathodic deposition from mixed nickel nitrate solutions (Co 5 mol%, La 5 mol%) exhibited durable electrochromism to at least 2000 cycles, while a binary composite hydroxide of $\beta(II)$ with 10% coprecipitated cobalt exhibited a stable electrochromic response up to 500 cycles. A binary composite of nickel hydroxide with lanthanum prepared by cathodic deposition from a mixed nitrate solution [35] showed increased cycling stability; however, the stability was tested only up to 180 cycles. A disadvantage of Ni(La)-hydroxide films is the lowering of the overpotential for the oxygen evolution reaction compared to that of undoped nickel hydroxide films [32].

The aim of this paper is to explain the increased cycling stability of Ni(La)-hydroxide films prepared via the sol-gel route. IR spectroscopy was used in order to detect the phases which develop during extensive cycling (up to 1802 cycles), and their appearance was correlated with the Bode scheme (Eq. 1). In addition, we evaluated the electrochromic properties of the films. Vibrational spectra assignment of Ni(La)-hydroxide films given here is based on our previous studies, and details of the NGIA (near-grazing incidence angle) reflection-absorption IR spectroelectrochemical methods can be obtained elsewhere [24, 26].

The second objective of this study is to obtain information about the effect of various cations, i.e., tetramethylammonium (TMA^+) and lithium (Li^+) ions, on the electrochromism of Ni(La)-hydroxide films. IR spectroscopy is very useful for the detection of intercalated species when these exhibit well-defined and characteristic vibrational bands in the frequency window, where vibrational groups of the parent film do not absorb. Stretching $\nu(CH_3)$ modes of TMA^+ ions appear in the range 3000–2800 cm^{-1}, which is free of the nickel hydroxide absorption. We have also tried to correlate our IR spectroscopy data with the results obtained by QCM coupled with cyclic voltammetry (CV) [19, 33, 36, 37].

Experimental

Preparation procedure

Thin films were prepared from nickel sulfate heptahydrate (Kemika, Croatia) and lanthanum acetate hydrate (Aldrich, Germany) precursors. First, a 1 M solution of $NiSO_4$ was precipitated with 4 M LiOH (Kemika, Croatia) until the pH reached 9. The green precipitate was thoroughly washed with deionised water and peptised with glacial acetic acid (Merck, Germany) to pH 4.5. At this stage, water and lanthanum acetate hydrate were added to the sols in an Ni:La molar ratio in the precursors of 20:1 and 10:1. Thin films were deposited using the dip-coating technique (pulling velocity 5 cm min^{-1}) onto SnO_2/F-coated glass (sheet resistance 10 Ω) and Pt bulk plate ($5 \times 2.5 \times 0.3$ cm^3) substrates. Prior to deposition, the surface active agent Teloksid (1 wt% in ethanol, TEOL Factory, Slovenia) was used as a wetting agent. Films thermally treated at various temperatures were tested, but the results reported herein refer only to the films with an Ni:La molar ratio of 10:1 and thermally treated at 300 °C for 15 or 60 min, since these films exhibited the highest colouring/bleaching changes and stability against cycling. The thickness of the films was from 30–50 nm per dipping.

Measurement techniques

Thickness measurements were performed using a Surface Profiler Alfa Step 200 with a maximum resolution of 0.5 nm per 100 nm. X-Ray Diffraction Analysis (XRD) was performed using a Philips PW 1710 X-Ray powder diffractometer with CuK_α radiation from 15 to 95° 2Θ in steps of 0025° 2Θ and 1 s per step. The films were carefully removed from the glass substrates, powdered, and the XRD spectra measured.

Ex-situ NGIA (near-grazing incidence angle) FT-IR spectra of thin films were obtained using a Perkin-Elmer Model 2000 spectrometer equipped with an NGIA reflectance accessory (Spectratech, UK). This technique allows reflection-absorption measurements of films deposited on highly reflecting substrates (Pt bulk plate) using P-polarised light at near-grazing incident conditions (80°). An Al-coated glass plate was used for background

measurements. Spectra were recorded at a resolution of 4 cm^{-1} in the range 4000–400 cm^{-1}. NGIA FT-IR spectra are expressed in the units of normalised reflectance ($\Delta R/R = 1 - R/R_0$) where R and R_0 correspond to the reflectance of the film and the substrate. The detailed background of this technique together with the interpretation of the longitudinal optical (LO) spectra can be found in our previous publications [24, 26].

Cyclovoltammetric (CV) and chronocoulometric (CC) measurements were performed at room temperature (20 $\pm$ 1 °C) using an EG&G PAR Model 273 computer-controlled potentiostat-galvanostat, driven by the 270 Electrochemical Analysis software. A three-electrode system and a Metrohm-type cell (140 ml of electrolyte) were employed. A Pt rod served as a counter electrode, an Ag/AgCl/KCl$_{sat}$ as a reference electrode (0.197 V) and a thin Ni(La)-hydroxide film on Pt bulk plate as a working electrode. The electrolyte comprised 0.1 M LiOH and 0.1 M tetramethylammonium hydroxide (TMAH – Fluka, Switzerland). A potential scan rate of 20 mVs^{-1} was used for the CV measurements.

In situ UV-VIS spectroelectrochemical measurements were made using a Hewlett-Packard 8452A Diode Array Spectrophotometer in the range 360–1100 nm. This was connected with the above-described EG&G PAR 273 system. A home-made three-electrode spectroelectrochemical transmission cell filled with 40 ml of 0.1 M LiOH was used in these investigations. For background measurements, a cell filled with only the electrolyte was used.

Results

Thermogravimetric measurements

Thermogravimetric measurements (Fig. 1) were made with air-dried Ni-hydroxide sols to which no lanthanum was added. Up to 700 °C, two distinct mass losses were observed, agreeing with previously published results [1, 2, 9]. The first mass loss appeared at 80 °C and is caused by the release of loosely bound water. The onset of the more abrupt mass loss, noted around 300 °C, is due to the removal of water and the decomposition of the carboxylate residues from the sol. This was proved by gas evolution measurements that showed the presence of water and CO$_2$ [26]. Beyond 330 °C, no decomposition of the sample was observed, confirming the formation of NiO (bunsenite) proved by XRD and IR measurements.
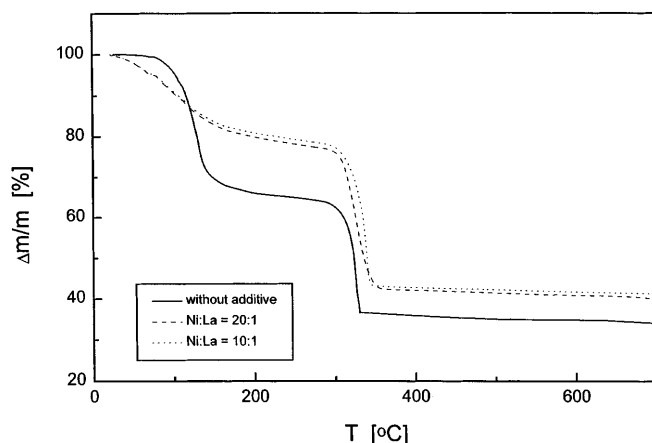
TG measurements of sols containing the lanthanum acetate precursor revealed a more continuous mass loss (Fig. 1). IR spectra of thermally treated samples for 15 and 60 min revealed the presence of water and sulfate groups. This is important for obtaining electrochromically active yet electrochemically stable films. Films in which all the water and sulfate moieties have been removed are electrochromically inactive [38, 39]. Ni(La)-hydroxide films are not as electrochromically active as undoped films, but, because of the longer heating times, a stronger network of the NiO phase is formed, which increases the electrochemical stability of Ni(La)-hydroxide film.

XRD measurements

Attempts to obtain XRD spectra of films prepared by single dipping cycle were unsuccessful owing to a too low signal. Even thick films (10 dipping cycles) did not reveal XRD peaks, which might be attributed to any of the expected peaks of the crystalline Ni(OH)$_2$ or NiO phases. We did not try to increase the number of dipping cycles. In general, when multiple dipped films are considered, the lower-lying film layers undergo successive heatings which may increase their crystallisation. In order to avoid the possible calcination of thick films, 30 single dipped films (2.5 × 5 cm^2) were prepared by heating at 300 °C for 15 min. Each film was then removed from the glass substrate, and the XRD spectrum of the collected powder was recorded (Fig. 2). This procedure was not repeated for films heated for 60 min at 300 °C because these films are difficult to remove from the glass.

The XRD spectrum of Ni(La)-hydroxide powder (molar ratio Ni:La = 10:1; 15 min at 300 °C) confirms the presence of NiO (bunsenite phase PDF No. 4-835)
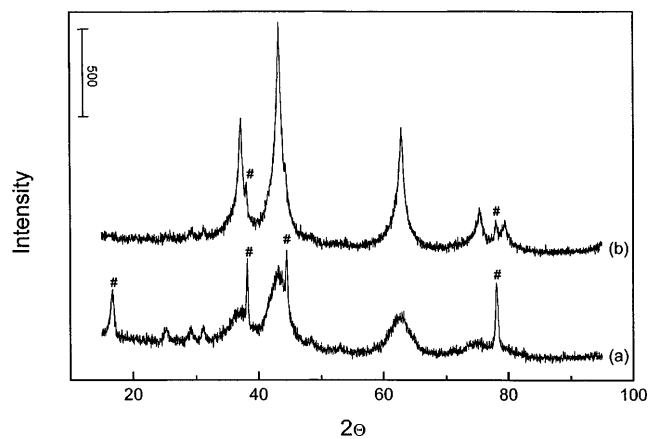

Fig. 1 TG curves of Ni- and Ni(La)-hydroxide powders obtained using the rate of temperature increase 10 °C min^{-1}

Fig. 2 XRD spectra of *a* powder obtained by stripping off Ni(La)-hydroxide films heated at 300 °C for 15 min and *b* as in *a* with the NiO standard added. # denotes the Al reflections from the sample holder

with crystalline grains of approximately 30 Å (Fig. 2). The IR spectra of the corresponding film and powder revealed that, besides NiO, the Ni(OH)$_2$ phase was present. The amount of the NiO phase in these films was estimated from an XRD spectrum of powdered films into which a known amount of NiO (Kemika, Croatia) had been added. The results showed that the films contained approximately 40% of the NiO phase, agreeing with the amount of crystalline NiO in Ni hydroxide films prepared either with organic [24] or Si [26] additions. From IR spectroscopic analysis of films and powders (not shown here), we found that the additional Ni(OH)$_2$ phase, which was not observed in XRD spectra, corresponds to the amorphous α(II)-Ni(OH)$_2$ phase. The extensive IR spectroscopic studies are reported in the literature [24, 26].

Electrochemical and electrochromic properties of films – in situ UV-VIS spectroelectrochemical measurements

The detection of ex situ IR spectra requires that the colour of the film is retained during the period when the IR spectroscopic measurements are made (~10 min). Thus, we examined the electrochromic properties of Ni(La)-hydroxide films (300 °C, 15 and 60 min) in a 0.1 M LiOH electrolyte to reveal how heating affects the colour retention of films and the differences between their EC responses. The results showed that the film heated for 15 min at 300 °C bleached in the open atmosphere in under 3 min, which meant that ex situ IR spectra of the coloured film could not be made. Therefore, we concentrated on film heated for 60 min, while the film heated for 15 min was analysed only to show the development of a stable electrochromic response (200 cycles).

The CV response of a 35-nm thick as-deposited film heated for 60 min (Fig. 3B) exhibits smaller currents and more pronounced current peaks than that of a 45-nm thick film heated for 15 min (Fig. 4B). This is caused by the greater amount of water, hydroxyl and carboxylate groups in the film heated for less time. The CV response of film heated for longer periods is similar to that of films prepared by an alternately dipping deposition technique [9] and by wet deposition from sols prepared from nickel nitrate and ethylene glycol [38]. Film obtained by heating for 15 min exhibits CV peaks resembling those of electrodeposited [10, 21] and sputtered [15, 16] films.

Cycling changes the CV response of both kinds of film (Figs. 3B, 4B). Particularly, the current peaks of film heated for 60 min become sharper with cycling, compared to those of film heated for 15 min, although, after 1400 cycles, film heated for 60 min still shows a smaller current density value than film heated for 15 min and cycled only 200 times. Cycling is accompanied by a distinct shift in E_p^{ox} from 0.61 V in the 100th cycle to 0.64 V in the 1400th cycle, while E_p^{red} retains its position at 0.32 V. A positive shift in the redox potential of the nickel hydroxide films has been often attributed to the formation of the β(II) phase [1, 33, 40].
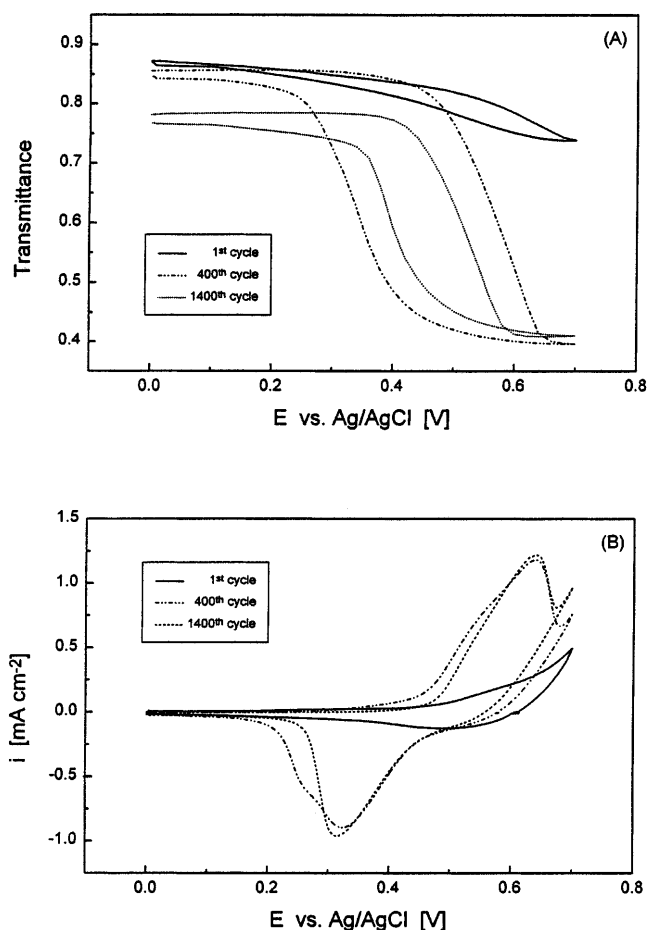

Fig. 3A Monochromatic transmittance changes (λ = 480 nm) and **B** cyclovoltammetric curves of 35-nm thick Ni(La)-hydroxide film with Ni:La molar ratio 10:1 heated at 300 °C for 60 min in 0.1 M LiOH. Scan rate was 20 mVs^{-1}. Transmittance was measured once per second

The most pronounced difference between the two types of film is in the monochromatic spectral transmittance (λ = 480 nm) of colouring/bleaching changes detected during CV measurements. Figure 4A shows how the colouring of the film, heated for 15 min, remains incomplete at the anodic vertex potential (0.7 V), and the film continues to colour during a reversal scan until a potential of 0.6 V is reached. Conversely, the full coloration of the film heated for 60 min (Fig. 3A) is achieved at the highest anodic potential (0.7 V). During the cathodic scan the latter film starts to bleach without a delay (at about 0.6 V), reaching the initial transmittance before the cathodic scan is completed, i.e., at 0.2 V (400th cycle) and 0.4 V (1400th cycle), respectively. In this respect, the film behaves analogously to nickel hydroxide films prepared by alternate-dipping deposition [9], thermal decomposition [20] and electrochemical deposition [41]. Conversely, the behaviour of the film heated for 15 min resembles that of sol-gel deposited films prepared with the addition of organics [24] and Si [26] and sputtered films [15, 16]. The differences between the two types of film also indicate that the rate of the
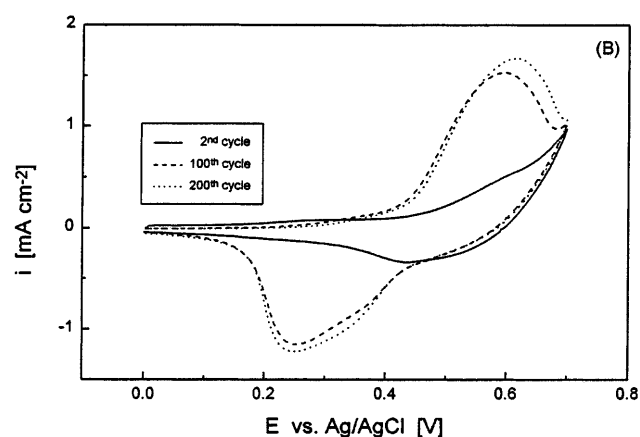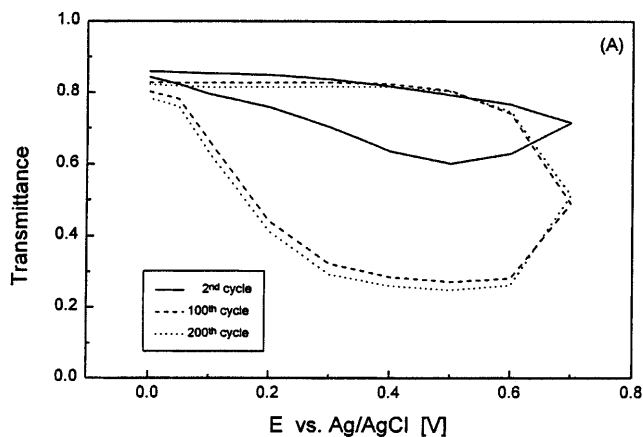
Fig. 4A Monochromatic transmittance changes (λ = 480 nm) and **B** cyclovoltammetric curves of 45-nm thick Ni(La)-hydroxide film with Ni:La molar ratio 10:1 heated at 300 °C for 15 min in 0.1 M LiOH. Scan rate was 20 mVs^{-1}. Transmittance was measured once per 5 s
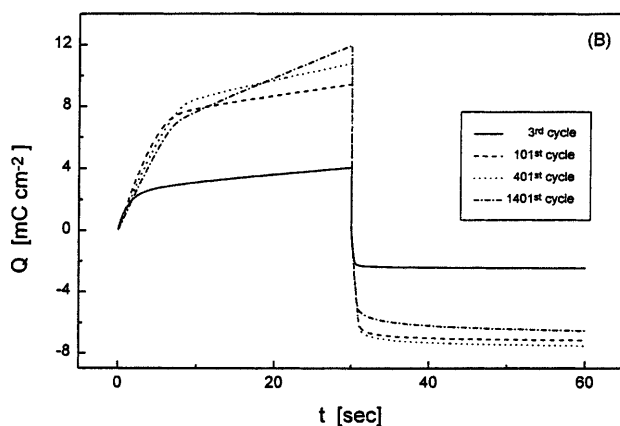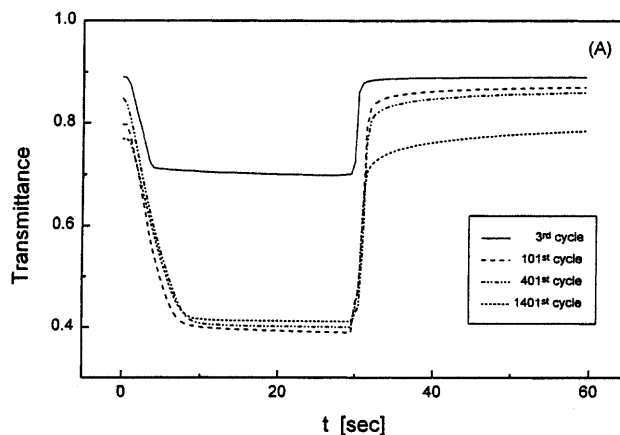
Fig. 5A Monochromatic transmittance changes (λ = 480 nm) and **B** chronocoulometric curves of 35-nm thick Ni(La)-hydroxide film with Ni:La molar ratio 10:1 heated at 300 °C for 60 min in 0.1 M LiOH. The film was coloured at 0.6 V for 30 s and bleached at –0.2 V for 30 s

electrochemical transformation in the film heated for 60 min is much higher than in the film heated for only 15 min. The lower transmittance in the coloured state of the film heated for 15 min is thought to be a result of the greater film thickness (45 nm) compared to the film heated for 60 min (35 nm).

Despite the difference in the monochromatic spectral transmittance changes (λ = 480 nm) detected during CV measurements (Figs. 3A, 4A), the colouring/bleaching changes of film heated for 60 min, obtained during charging/discharging at limiting potentials (i.e. –0.2 V and 0.6 V) (Fig. 5A), are not so different from those of the film heated for 15 min (Fig. 6A). This reflects the lower sensitivity of this method for detecting the differences in the colouring/bleaching kinetics of films as a function of their structure. Both films show oxygen evolution (Figs. 5B, 6B), which is obvious from the continuous increase in charge after the transmittance reached a plateau ($\sim$7 s) and the higher charging values that the films develop during the anodic scans [32]. Additionally, the Q_{cath}/Q_{anodic} ratio detected for the film

heated for 60 min decreases from 0.76 in the 101st cycle to 0.55 in the 1401st cycle. A similar Q_{cath}/Q_{anodic} ratio was noted for the film heated for 15 min, i.e., 0.73 in the 101st cycle and 0.74 in the 201st cycle.

The spectral electrochromic response is depicted in Figs. 7 and 8. Both types of film exhibit high transparency in the as-deposited state ($>80\%$). This agrees with other nickel hydroxide films where the amount of the absorbing NiO (bunsenite) phase is small or completely absent [10, 34, 35]. The UV-VIS spectra recorded after charging/discharging for 30 s at limiting potentials (i.e., 0.6 V and –0.2 V) reveal an electrochromic response that gradually develops with cycling, attaining persistent values after 100 cycles. Extensive cycling (up to 1400 cycles) performed for the film heated for 60 min (Fig. 7A) leads to a decrease in the transmittance in its bleached state, while the transmittance of the coloured state remains constant. In this respect, the behaviour of the film resembles that of sol-gel-derived Ni(Si)-hydroxide films cycled 200 times [26] and clearly indicates the retention of the Ni^{3+}-absorbing phase in the
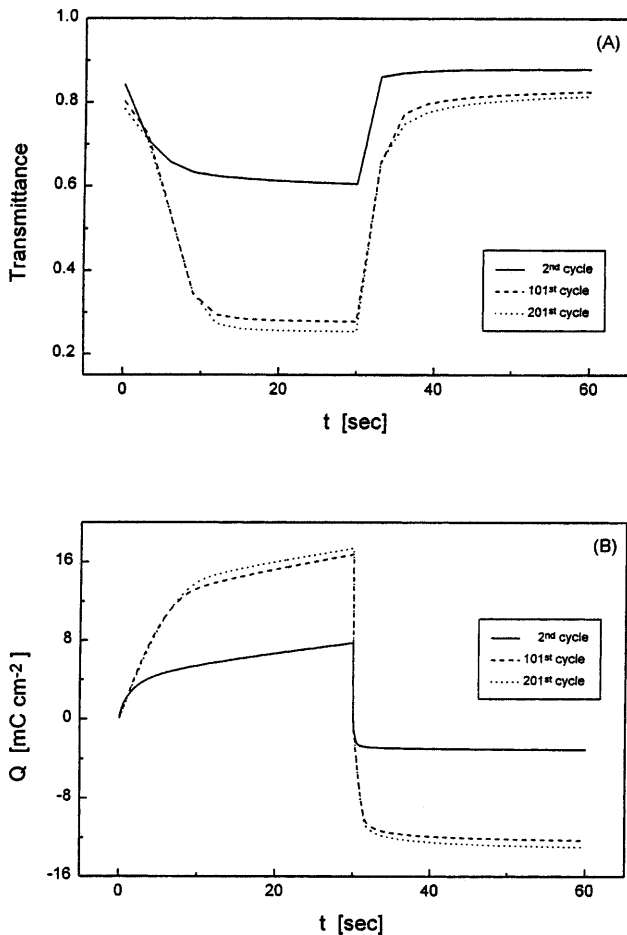
Fig. 6A Monochromatic transmittance changes (λ = 480 nm) and **B** chronocoulometric curves of 45-nm thick Ni(La)-hydroxide film with Ni:La molar ratio 10:1 heated at 300 °C for 15 min in 0.1 M LiOH. The film was coloured at 0.6 V for 30 s and bleached at −0.2 V for 30 s

Fig. 7A Transmittance spectra and **B** optical density changes $\Delta OD_{480 \text{ nm}}$ of 35-nm thick Ni(La)-hydroxide film with Ni:La molar ratio 10:1 heated at 300 °C for 60 min in 0.1 M LiOH. The film was initially coloured at 0.6 V for 30 s and bleached at −0.2 V for 30 s

bleached state. Conversely, films obtained by alternate-dipping deposition [9] steadily increase the colouring/bleaching changes on account of the decreased tansmittance of films in their coloured state. Ni-hydroxide films containing organics [24] behave differently, at least up to 200 cycles, and exhibit a decrease in transmittance in the bleached and coloured states with cycling. It is apparent that the persistent electrochromic response largely depends on the preparation of the film.

The effects of different heating times on the electrochromism of the films cannot be determined from the transmittance spectra (Figs. 7, 8). This is because the thicknesses of the two kinds of film differ by about 25%. When optical densities and film thickness ($\Delta OD_{480 \text{ nm}}/d$) are considered, the results reveal that the longer heating time only slightly decreases the electrochromic response, lowering the $\Delta OD_{480 \text{ nm}}/d$ values of the films (Table 1). Prolonged cycling decreases the $\Delta OD_{480 \text{ nm}}/d$ values from 0.009 nm^{-1} (101st cycle) to 0.007 nm^{-1} (1401st cycle) for a 60-min heated film, which is a consequence of a drop in the transmittance of the film in the bleached state. It should be noted that our films exhibit similar
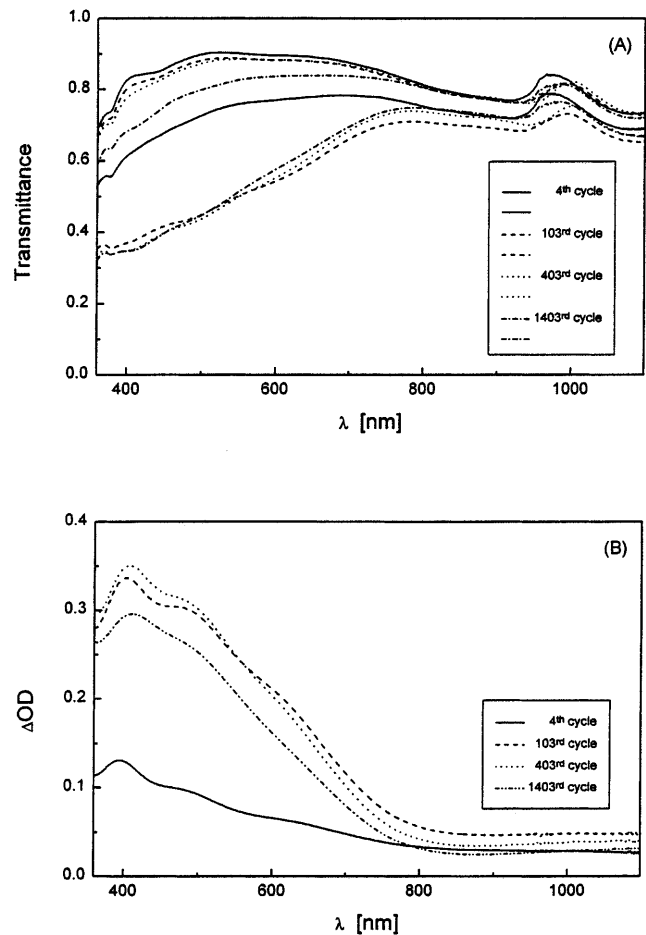
optical density values compared to sputtered and e-beam evaporated films [4].

The coloration efficiency (Table 1), defined as the change in optical density per unit of inserted charge ($\Delta OD/\Delta Q$ in cm^2 C^{-1}), is 27.5 cm^2 C^{-1} in the 101st cycle for a film heated for 15 min, while a film heated for 60 min at the same cycle exhibits a smaller coloration efficiency value (20.4 cm^2 C^{-1}). The two values are in good agreement, albeit somewhat smaller than those reported for nickel hydroxide films prepared by other deposition methods [4].

Ex situ NGIA spectroelectrochemical measurements

Ex situ NGIA IR spectra of Ni(La)-hydroxide films (Ni:La molar ratio 10:1, 300 °C, 15 and 60 min) were recorded in order to obtain an insight into the structural changes caused by charging/discharging of the films. Films, deposited on Pt bulk plate, were potentially cycled between 0.1 V and 0.65 V in 0.1 M LiOH and 0.1 M TMAH electrolytes, respectively. NGIA IR
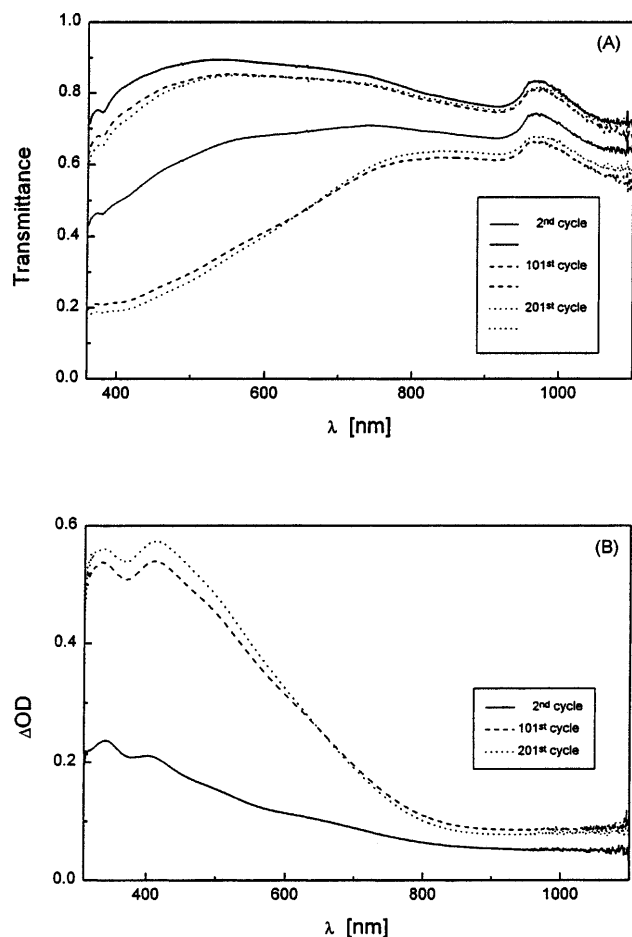
Fig. 8A Transmittance spectra and **B** optical density changes $\Delta OD_{480\,nm}$ of 45-nm thick Ni(La)-hydroxide film with Ni:La molar ratio 10:1 heated at 300 °C for 15 min in 0.1 M LiOH. The film was initially coloured at 0.6 V for 30 s and bleached at −0.2 V for 30 s

spectra were measured after various numbers of cycles: 6, 101, 201, 401, 601, 1402 and 1802. Before recording the NGIA IR spectra, the films were chronocoulometrically coloured at 0.6 V or bleached at −0.2 V for 30 s,

removed from the electrochemical cell, rinsed with deionised water and dried in a stream of hot air. The Ni(La)-hydroxide films heated for 60 min at 300 °C retained their colour, which made it possible to detect the NGIA IR spectra of coloured states, while the films heated for 15 min bleach quickly (< 3 min), preventing the ex situ NGIA IR measurements of this type of film in the coloured state.

It should be noted that CO_2 bands (2350 cm^{-1}) appear in ex situ NGIA IR spectra with different intensities owing to the variations in CO_2 concentration in the sample compartment of the spectrometer. Even though this might be avoided by using appropriate purging, we made our measurements without purging with N_2 gas because the CO_2 bands neither interfere with the other vibrational modes nor influence the reproducibility of the results.

NGIA IR spectra of as-deposited Ni(La)-hydroxide films (Ni:La molar ratio 10:1) prepared by thermal treatment for 60 min at 300 °C (Figs. 9a, 10a) show the presence of sulfate groups $\nu(SO_4^{2-})$ at 1150 cm^{-1} and $\delta(SO_4^{2-})$ at 630 cm^{-1}, a broad $\nu(OH...O)$ stretching mode in the frequency range 3600–3000 cm^{-1}, $\delta(H_2O)$ deformation at 1651 cm^{-1} and a small amount of adsorbed CO_3^{2-} species (1600–1300 cm^{-1}). The $\nu(Ni^{2+}\text{-O})$ stretching mode that signals the presence of bunsenite appears around 500 cm^{-1}, while the $\delta(Ni^{2+}\text{-OH})$ mode belonging to the $\alpha(II)$ phase becomes apparent only when the films have been in contact with the electrolyte at 670 cm^{-1} (Figs. 9, 10). The same is also true for the remaining band at 720 cm^{-1}, which belongs to the $\gamma(H_2O)$ rocking mode, confirming the hydration of films.

By the 6th cycle, the anodically/cathodically charged film at 0.6 V and −0.2 V in 0.1 M LiOH exhibits the almost complete removal of sulfate species. This may be judged from the decrease in the intensity of the SO_4^{2-} stretching band at 1150 cm^{-1} (Fig. 9b,c). According to Faure et al. [2, 3, 27] and our previous results [24, 26], this mode is attributed to the SO_4^{2-} ions free of H-bonding. The remaining bands in the sulfate region have much lower intensities and were ascribed to bi- and

Table 1 Optical density $\Delta OD_{480\,nm}$ and coloration efficiency η values obtained for Ni(La)-hydroxide films with Ni:La molar ratio 10:1 heated at 300 °C for 15 and 60 min during cycling in 0.1 M LiOH

Number of cycle	$\Delta OD_{480\,nm}$	$\Delta OD_{480\,nm}/d$ (nm^{-1})	$\Delta OD_{480\,nm}/Q_A$ (cm^2 C^{-1})	$\Delta OD_{480\,nm}/Q_C$ (cm^2 C^{-1})	$\Delta OD_{480\,nm}/Q_A d$ (cm^2 C^{-1} nm^{-1})	$\Delta OD_{480\,nm}/Q_C d$ (cm^2 C^{-1} nm^{-1})
Molar ratio Ni:La = 10:1, 300 °C for 15 min, d_{film} = 45 nm						
2	0.15	0.003	18.9	−47.4	0.42	−1.05
101	0.46	0.010	27.5	−37.6	0.61	−0.84
201	0.49	0.010	28.2	−37.8	0.63	−0.84
Molar ratio Ni:La = 10:1, 300 °C for 60 min, d_{film} = 35 nm						
3	0.10	0.003	15.3	−25.1	0.44	−0.72
101	0.30	0.009	20.4	−26.9	0.58	−0.77
201	0.32	0.009	20.2	−27.0	0.58	−0.77
401	0.31	0.009	18.4	−26.4	0.53	−0.75
1001	0.27	0.008	14.0	−25.8	0.40	−0.74
1401	0.26	0.007	14.0	−25.7	0.40	−0.73

Fig. 9 NGIA IR reflection-absorption spectra ($\Delta R/R$) of an Ni(La)-hydroxide film (Ni:La molar ratio 10:1, 300 °C for 60 min) obtained during cycling in 0.1 M LiOH: **a** as-deposited, **b, d, f, h, j, l** (*upper curves*) coloured states and **c, e, g, i, k, m** (*lower curves*) bleached states. Before being analysed, the film was chronocoulometrically coloured at 0.6 V for 30 s and bleached at −0.2 V for 30 s (Here, and elsewhere, * indicates CO_2 absorption due to insufficient purging)
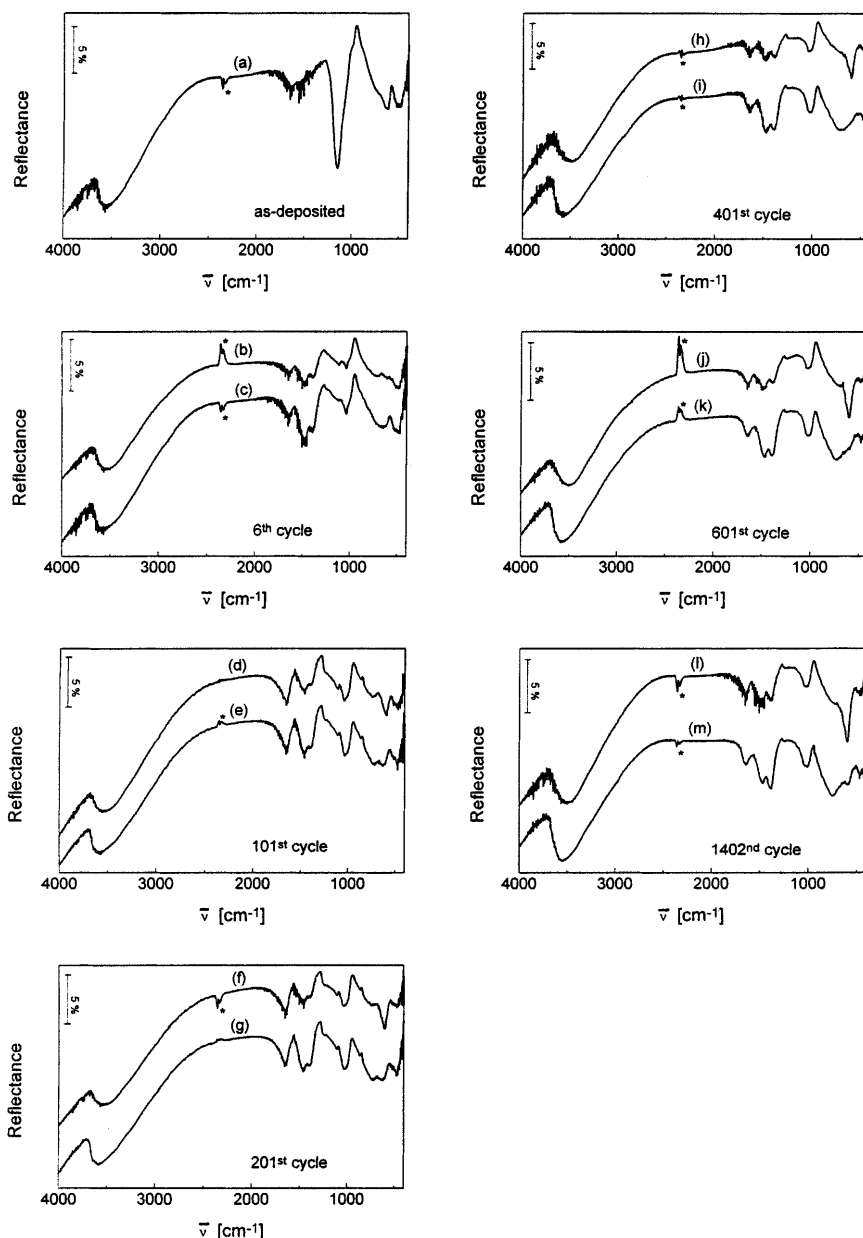

monodentately bounded SO_4^{2-} ions to Ni ions [2, 24]. The shape of the $\delta(Ni^{2+}\text{-OH})$ and $\gamma(H_2O)$ bands in the IR spectra of bleached film is atypical for the $\beta(II)$ phase, agreeing with the absence of the sharp hydroxyl $\nu(OH)$ stretching band at 3645 cm^{-1}. This suggests that the $\alpha(II)$ phase is the prevailing phase in the film. The expected $\beta(II)$ phase does not develop with cycling. Even with prolonged cycling (up to 1400 cycles), the vibrational bands attributed to the $\beta(II)$ phase did not develop. In the IR spectra of the cycled film the intensity of the $\nu(OH...O)$ stretching mode, in the range 3600–3000 cm^{-1}, increases in intensity ($\sim$30%), indicating hydration of the film. The frequency of the water-deformational band (1651 cm^{-1}), the carbonate stretchings (1300–1600 cm^{-1}) and the $\nu(Ni^{2+}\text{-O})$, (bunsenite at

476 cm^{-1}) mode do not shift or show any change in intensity in the IR spectra of cycled films.

In the IR spectra of anodically charged film, the most salient feature is the appearance of the $\nu(Ni^{3+}\text{-O})$ stretching mode (600 cm^{-1}), which increases in intensity with cycling. This clearly shows the development of the $\gamma(III)$ phase. Reproducibility of measured IR spectra of films in charged and discharged states is good, bringing about nearly identical spectra of films prepared under the same conditions. The absolute intensities of the reflection-absorption LO bands vary by a few percent; however, the relative intensities of the observed bands are reproducible. The variations in the absolute intensity are due to the non-homogeniety of the film surface or the film surface area. Additionally, mechanical defects

Fig. 10 NGIA IR reflection-absorption spectra ($\Delta R/R$) of an Ni(La)-hydroxide film (Ni:La molar ratio 10:1, 300 °C for 60 min) obtained during cycling in 0.1 M TMAH: **a** as-deposited, **b, d, f, h, j, l, n** (*upper curves*) coloured states and **c, e, g, i, k, m, o** (*lower curves*) bleached states. Before being analysed, the film was chronocoulometrically coloured at 0.6 V for 30 s and bleached at −0.2 V for 30 s
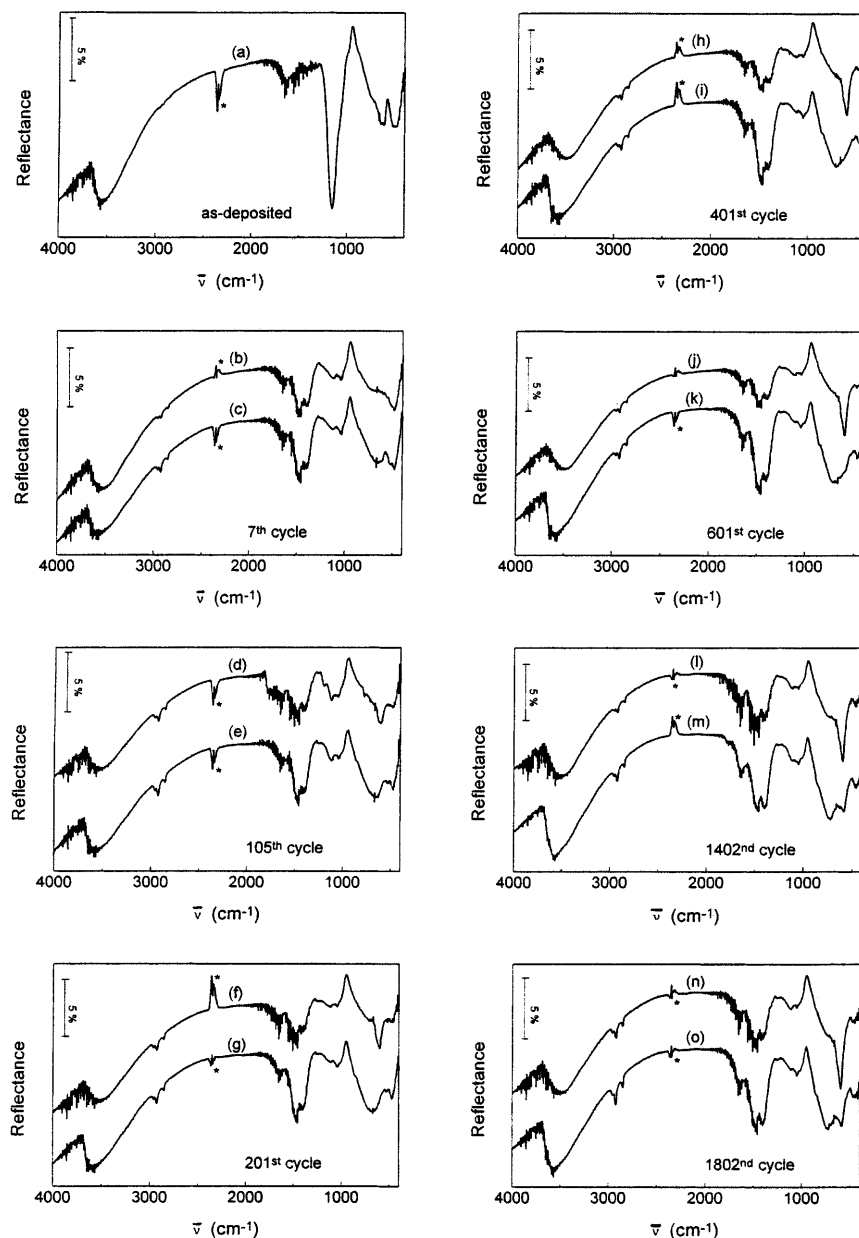
might also appear during the cleaning and drying of the films when taken from the electrochemical cell prior to IR spectra detection. Details of the relationship between the observed longitudinal optical (LO) modes in the NGIA IR spectra with the transversal modes (TO) of films in the coloured and bleached states and the LO and TO vibrational spectra of model phases [α(II), γ(III), β(II), β(III)] have been reported previously [24, 26].

Ex situ NGIA FT-IR spectroscopic analysis (see above) was repeated for the Ni(La)-hydroxide film (Ni:La molar ratio 10:1, 300 °C, 60 min) in a 0.1 M TMAH electrolyte (Fig. 10). A typical spectrum of a cycled film (1802nd cycle) together with a detailed vibrational band assignment is given in Fig. 11. TMA$^+$ cations absorb in the region 3000–2800 cm^{-1} (CH$_3$ stretchings), while the C$_4$N stretching and deformational

modes occur at 950 and 450 cm^{-1} [42]. The CH$_3$ bending and rocking modes are quite weak and appear between 1500–1400 cm^{-1} and 1300–1100 cm^{-1}, respectively. Therefore, we concentrated on the v(CH$_3$) modes appearing in the spectral range free of interfering vibrations of the Ni(La)-hydroxide film. Other TMA$^+$ modes are blurred by stretching v(CO$_3^{2-}$) and the remaining v(SO$_4^{2-}$) modes of the film.

The IR spectra of the Ni(La)-hydroxide film in 0.1 M TMAH (Fig. 10) are almost identical to those obtained by cycling in 0.1 M LiOH (Fig. 9), with the exception that the v(CH$_3$) modes gradually increase in their intensity when cycled in TMAH. The most important distinction between the two sets of IR spectra is the appearance of a pronounced v(Ni^{3+}-O) mode at 600 cm^{-1} in the spectra of bleached films cycled 1802

and 1402 times in 0.1 M TMAH (Fig. 10m, o). This indicates that the retention of the γ(III) phase in the bleached states is more accentuated when the film is cycled in the 0.1 M TMAH electrolyte.

Discussion

Using ex situ IR and in situ UV-VIS, we found that the cycling stability of Ni(La)-hydroxide films is due to the α(II)/γ(III) phase transformation. This has been well proven from the detailed vibrational analysis of the measured IR spectra of bleached and coloured states, which have been interpreted as α(II) and γ(III) phases [24, 26]. The absence of the β(II) phase is crucial for ruling out the β(II)/β(III) redox changes. IR spectroscopic evidence for the absence of this phase is unambiguous, since the hydroxyl v(OH) band at 3645 cm^{-1} (characteristic of the β(II) phase) is not found in the ex situ IR spectra of bleached states in either of the electrolytes (Figs. 9, 10). Additional evidence for the existence of the α(II) phase is the observed blue frequency shift of the δ(Ni^{2+}-OH) stretching mode, which gradually shifts from 646 cm^{-1} (2nd cycle) to 727 cm^{-1} (1802nd cycle) when cycled in 0.1 M TMAH. The reverse frequency shift with cycling would be observed if the β(II) phase was formed from the initial α(II) phase [24, 26].

The band appearing at 600 cm^{-1} is characteristic of the γ(III) phase and not of the β(III) phase which would appear at 593 cm^{-1} [24, 26]. However, in the spectra of coloured states (Figs. 9, 10), we did not find the "free" hydroxyl band at 3645 cm^{-1}, which was found in the in situ Raman spectra [43] and IR spectra of Ni(Si)-hydroxide films [26]. The presence of this band in the ex situ IR spectra of coloured states would signal the electrochemically irreversible γ(III) phase with an expanded hydrated structure.

Indirectly, the presence of the fully hydrated γ(III) phase was ascertained from the measured v(OH...O) band intensities, which increase by 30% in the IR spectra of a cycled film (1802 cycles in 0.1 M TMAH) compared to the as-deposited film or film cycled just 6 times. This suggests that the hydrated γ(III) phase is formed with cycling, despite being undetected in the IR spectra of coloured states (Figs. 9 l; 10 l, n; 11). This also agrees with the in situ UV-VIS spectroelectrochemical measurements, where a decrease in transmittance of the bleached state appears in the 1403rd cycle (Fig. 7). In addition, in the IR spectra of the bleached films (Figs. 9m; 10m, o; 11) cycled more than 1400 cycles, the v(Ni^{3+}-O) stretching at 600 cm^{-1} appears, indicating the presence of the Ni^{3+} absorbing phase.

To determine the kind of species involved in mass transport, we measured the relative integral intensities of the v(CH$_3$) modes attributed to the TMA$^+$ ions in the IR spectra of the film cycled in 0.1 M TMAH (Figs. 10, 11). The integral intensities were determined directly from

the reflection-absorption spectra of charged and discharged film by calculating the areas below the v(CH$_3$) bands in the frequency range $v_1 = 2835$ to $v_2 = 2990$ cm^{-1}. The base line was obtained by linear extrapolation of the reflection-absorption response ($\Delta R/R$) between the limiting frequencies in the spectral range of the v(CH$_3$) bands. The integral intensities were expressed relative to the maximal integral intensity of the v(CH$_3$) bands, obtained from the spectrum of a bleached Ni(La)-hydroxide film cycled 1802 times in 0.1 M TMAH (Fig. 10o). The results show (Fig. 12) that after the 6th oxidation cycle the coloured film contained a small amount of TMA$^+$ ions. Subsequent reduction immediately increased the relative integral intensity of the v(CH$_3$) bands, indicating the immediate incorporation of TMA$^+$ ions during the cathodic cycle. When the 105th scan is completed, the relative integral intensity further increases, suggesting the accumulation of TMA$^+$ ions in the film with further cycling. Stabilisation of the amount of incorporated TMA$^+$ ions is achieved between the 401st and 1402nd cycle, after which the amount of TMA$^+$ ions again starts to increase. This increase is the same in both the coloured and bleached states.

A closer examination of the ex situ IR spectra of film cycled in 0.1 M TMAH (Figs. 10, 11) reveals that up to the 105th cycle the 600 cm^{-1} band attributed to the v(Ni^{3+}-O) stretching mode is not fully developed, but is more pronounced in the spectrum of a film cycled 201 times. From the 401st up to the 601st cycle, the v(Ni^{3+}-O) band changes only slightly. In the IR spectra obtained during the 601st cycle and the 1402nd cycle the v(Ni^{3+}-O) stretching band also starts to appear in the spectra of bleached states. This band became even more pronounced in the IR spectra of film cycled 1802 times.

It is apparent that a close correlation exists between the changes in the v(CH$_3$) band intensities (Fig. 12) and
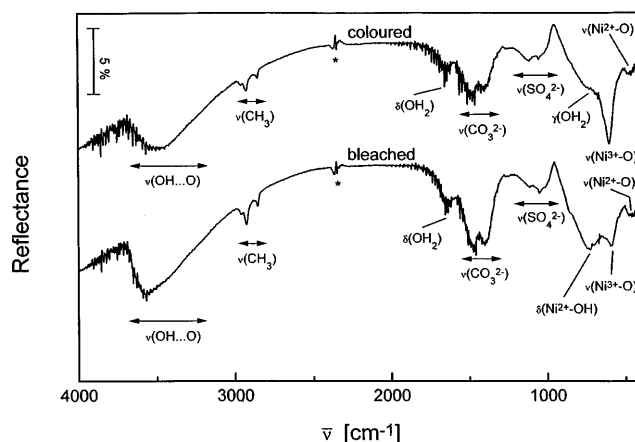

Fig. 11 NGIA IR reflection-absorption spectra ($\Delta R/R$) of an Ni(La)-hydroxide film (Ni:La molar ratio 10:1, 300 °C for 60 min) obtained during cycling in 0.1 M TMAH (1802nd cycle). Before being analysed, the film was chronocoulometrically coloured at 0.6 V for 30 s and bleached at −0.2 V for 30 s
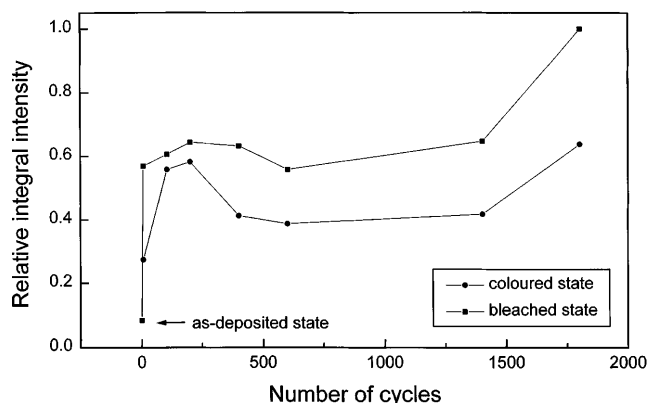
48

Fig. 12 The relative integral intensity of the $\nu(CH_3)$ stretching vibrations of TMA$^+$ ions in the Ni(La)-hydroxide film

the changes in the $\nu(Ni^{3+}\text{-O})$ stretching band observed in the IR spectra of the film (Figs. 10, 11). The amount of incorporated/extracted TMA$^+$ ions follows the development of the film structure, changing from the initial $\gamma(III)$ phase to more expanded $\gamma(III)$ phase. After the 1402nd cycle, the amount of TMA$^+$ ions in the film increases abruptly and is related to the formation of the highly hydrated, expanded and electrochemically irreversible $\gamma(III)$ phase. It is reasonable to suspect that further cycling would lead to the destruction of the film due to its full transformation to the more expanded and hydrated $\gamma(III)$ phase.

The presence of TMA$^+$ ions in our film agrees with the findings of Cordoba-Torresi et al. [36]. They assumed, on the basis of quartz crystal microbalance (QCM) measurements, that an appreciable amount of hydrated alkali ions are incorporated into the films, leading to their accumulation during cycling. Our results, however, do not confirm the behaviour of the Ni-hydroxide film prepared by Mo et al. [33], who found that composite Ni/Co-hydrous oxide films show a decrease in mass during the cathodic scan. In our films we observed the uptake of TMA$^+$ ions during the cathodic scan, though we cannot quantitatively evaluate the extent to which the deintercalation of OH$^-$ ions contributes to the bleaching process. Unfortunately, it is not possible to make any further correlation between our results based on IR spectroelectrochemical studies with those obtained by QCM of the composite Ni/Co-hydrous oxide films [33].

Conclusions

The sol-gel route is a versatile technique for obtaining composite Ni(La)-hydroxide films. Increasing the thermal treatment time of as-deposited xerogel films significantly improves the mechanical and abrasion resistance properties of deposited films without causing a deterioration in their electrochromic response.

The CV response of the films heated for 60 min at 300 °C resembled those prepared by the alternate-dipping deposition technique [9], albeit they were obtained with longer heating times and temperatures higher than 200 °C. The same was also found for the in situ UV-VIS monochromatic spectral transmittance changes that the Ni(La)-hydroxide films exhibit during subsequent colouring and bleaching.

The addition of lanthanum improved cycling stability. In situ UV-VIS and ex-situ NGIA IR revealed the transitions between the $\alpha(II)$ and the $\gamma(III)$ phases during the oxidation/reduction cycles in film cycled up to 1802 cycles, without the transformation to the $\beta(II)/\beta(III)$ redox pair.

The detection of the vibrational stretching $\nu(CH_3)$ modes of TMA$^+$ ions in the film during prolonged cycling proved the accumulation of cations. The decrease of the EC response of the film in the 1402nd cycle was attributed to the partial development of a more hydrated $\gamma(III)$ phase, which, according to its electrochemical irreversibility, causes a decrease in the EC response of cycled film by decreasing the transmittance of the film in the bleached state. The presence of this hydrated $\gamma(III)$ phase was supported by the appearance of the $\nu(Ni^{3+}\text{-O})$ stretching mode at 600 cm^{-1} in the IR spectra of bleached states. Finally, these results have shown the importance of a combined electrochemical and spectroelectrochemical approach to the investigation of the electrochemical and electrochromic properties of sol-gel-derived Ni(La)-hydroxide films. Incorporation of other dopants into Ni-hydroxide film is planned in order to assess their role in cycling stability.

References

1. Oliva P, Leonardi J, Laurent JF, Delmas C, Braconnier JJ, Figlarz M, Fievet F, de Guibert A (1982) J Power Sources 8: 229
2. Faure C, Delmas C, Fouassier M (1991) J Power Sources 35: 279
3. Faure C, Borthomieu Y, Delmas C, Fouassier M (1991) J Power Sources 36: 113
4. Granqvist CG (1995) Handbook of inorganic electrochromic materials. Elsevier, Oxford
5. Scrosati B (1994) In: Lipkowski J, Ross PN (eds) Electrochemistry of novel materials. VCH, New York, pp 111–140
6. Granqvist CG (1995) Handbook of electrochromic materials. Elsevier, Oxford, p 473
7. Orel B, Lavrenčič Štangar U (1994) J Electrochem Soc 141: L127
8. Orel B, Lavrenčič Štangar U, Opara U, Gaberšček M, Kalcher K (1995) J Mater Chem 5: 617
9. Fantini MCA, Bezerra GH, Carvalho CRC, Gorenstein A (1991) SPIE 1536: 81
10. Yu PC, Lampert CM (1989) Sol Energy Mater 19: 1
11. Bode H, Dehmelt K, Witte J (1966) Electrochim Acta 11: 1079
12. Le Bihan S, Figlarz M (1972) J Cryst Growth 13–14: 458
13. Kober FP (1965) J Electrochem Soc 112: 1064

14. Kober FP (1967) J Electrochem Soc 114: 215
15. Estrada W, Andersson AM, Granqvist CG, Gorenstein A, Decker F (1991) J Mater Res 6: 1715
16. Andersson AM, Estrada W, Granqvist CG, Gorenstein A, Decker F (1990) SPIE 1272: 96
17. Gorenstein A, Decker F, Estrada W, Esteves C, Andersson AM, Passerini S, Pantaloni S, Scrosati B (1990) J Electroanal Chem 277: 277
18. Lyman NR, Habibi HP (1988) SPIE 1016: 63
19. Nemetz A, Temmink A, Bange K, Cordoba de Torresi S, Gabrielli C, Torresi R, Hugot-Le Goff A (1992) Sol Energy Mater Sol Cells 25: 93
20. Torresi RM, Vazquez V, Gorenstein A, Cordoba de Torresi SI (1993) Thin Solid Films 229: 180
21. Yu PC, Nazri G, Lampert CM (1987) Sol Energy Mater 16: 1
22. Nazri G, Corrigan DA, Maheswari SP (1989) Langmuir 5: 17
23. Lampert CM, Caron-Popowich RS (1989) SPIE 1149: 56
24. Šurca A, Orel B, Pihlar B, Bukovec P (1996) J Electroanal Chem 408: 83
25. Šurca A, Orel B, Pihlar B (1997) J Sol-Gel Sci Techn 8: 743
26. Šurca A, Orel B, Cerc-Korošec R, Bukovec P, Pihlar B, (1997) J Electroanal Chem 433: 57
27. Faure C, Delmas C, Willmann P (1991) J Power Sources 35: 263
28. Faure C, Delmas C, Willmann P (1991) J Power Sources 36: 497
29. Delmas C, Faure C, Borthomieu Y (1992) Mater Sci Eng B 13: 89
30. Demourgues-Guerlou L, Delmas C (1993) J Power Sources 45: 281
31. Kamath PV, Dixit M, Indira L, Shukla AK, Kumar VG, Munichandraiah N (1994) J Electrochem Soc 141: 2956
32. Corrigan DA, Bendert RM (1989) J Electrochem Soc 136: 723
33. Mo Y, Hwang E, Scherson DA (1996) J Electrochem Soc 143: 37
34. Corrigan DA (1992) Sol Energy Mater Sol Cells 25: 293
35. Corrigan DA, Carpenter MK (1990) In: Lampert CM, Granqvist GC (eds) Large-area chromogenics, vol IS4. SPIE Opt Energ Press, Bellingham, USA, pp 298–312
36. Cordoba-Torresi SI, Gabrielli C, Hugot-Le Goff A, Torresi R (1991) J Electrochem Soc 138: 1548
37. Bernard P, Gabrielli C, Keddam M, Takenouti H, Leonardi J, Blanchard P (1991) Electrochim Acta 36: 743
38. Miki T, Yoshimura K, Tai Y, Tazawa M, Jin P, Tanemura S (1993) 3rd Int Conf Adv Mat, Tokyo, Japan, 31 August–4 September, Paper N° KP12
39. Cordoba-Torresi SI, Hugot-Le Goff A, Joiret S (1991) J Electrochem Soc 138: 1554
40. Visscher W, Barendrecht E (1983) J Electroanal Chem 154: 69
41. Fantini M, Gorenstein A (1987) Sol Energy Mater 16: 487
42. Brbot-Šaranović B, Orel B, Hadži D (1985) Phase Trans 5: 151
43. Johnston C, Graves PR (1990) Appl Spectrosc 44: 105